
Sutra: Tensor-Op RNNs as a Compilation Target for Vector Symbolic Architectures

Anonymous Author(s)

Affiliation

Address

email

1

2 Abstract

3 **Sutra** is a typed, purely functional programming language whose compiled forward pass is a Py-
4 Torch neural network. The compiler beta-reduces the whole program (primitives, control flow,
5 string I/O) to a fused tensor-op graph: rotation binding, unbind, bundle, polynomial Kleene three-
6 valued logic, and tail-recursive loops all lower to tensor operations on a frozen embedding substrate,
7 with the only remaining host-side control flow a thin tick-loop that breaks when a halt scalar satu-
8 rates. The Kleene connectives are Lagrange-interpolated polynomials exact on the $\{-1, 0, +1\}$ truth
9 grid; rotation binding doubles as the language's hash-map primitive (Haar-orthogonal role rotations
10 seeded by content hash). The substrate is the architecture target: swap the embedding model and the
11 same source recompiles against a different geometry.

12 The validation is a single fact testable two ways. (1) The same program runs on four frozen em-
13 bedding substrates spanning two modalities (three text encoders: nomic-embed-text, all-minilm,
14 mxbai-embed-large, and one protein language model: ESM-2) and decodes bundles at 100% ac-
15 curacy through width $k=8$ on every one, where the textbook Hadamard product has already col-
16 lapsed (2.5% on mxbai-embed-large, 7.5% on all-minilm); single-cycle bind/unbind round-trips at
17 $\approx 1.5 \times 10^{-15}$. A Sutra program's inputs and outputs are embeddings in the substrate's vector space;
18 a compile-time codebook handles string literals at the source level and nearest-string lookup at the
19 output boundary. (2) PyTorch autograd flows through the compiled graph end-to-end: a symbolic
20 if-then program of fuzzy rules over 20 classes / 992 words, with a rule tree nineteen ANDs deep,
21 trains from random init (4%; chance = 5%) to 95% within 50 epochs and holds through 300 without
22 any modification to the symbolic source. Gradient descent moves the embeddings the rules evaluate
23 against, leaving the rule graph itself untouched.

24 This collapses the boundary between writing a logic program and training a neural network: one
25 artifact, two interpretations.

26

27 1 Introduction

28 A frozen embedding model maps strings (or amino-acid sequences, or any other input the model
29 was trained on) into a deterministic continuous vector space. Given such a substrate, two technical
30 questions follow:

- 31 1. **Which operations on these embeddings are reliable enough to be used as primitives of**
32 **a compositional algebra over the substrate's vector space?**
- 33 2. **What is the correct binding operation?** Hyperdimensional computing's textbook bind
34 operators (Hadamard product, circular convolution) were derived assuming hypervectors

35 drawn from a controlled random distribution. Frozen LLM embeddings are not such a
36 distribution. §3.2 measures four substrates and reports that rotation binding decodes at
37 100% accuracy through bundle widths where Hadamard has already collapsed.

38 This paper answers both questions in the form of a working programming language, **Sutra**, whose
39 primitives are these consolidated operations and whose compiled forward pass is a PyTorch neural
40 network. The naming: **Sutra** is the Sanskrit *sūtra* (thread, rule, aphorism), the term for Pāṇini's
41 foundational Sanskrit grammar.

42 1.1 Contributions

43 The four core technical contributions of this paper are:

44 1. **Polynomial fuzzy logic via Lagrange interpolation of Kleene's three-valued truth tables.** The truth axis encodes $T = +1$, $U = 0$, $F = -1$. On the discrete $\{-1, 0, +1\}$
45 grid, the Kleene connectives are AND = min, OR = max, NOT = $- \cdot$. The min/max
46 forms (the standard Gödel t-norm/t-conorm choice; Hájek 1998) are non-differentiable at
47 the diagonal $a = b$, which breaks gradient flow when connectives compose with the tensor-
48 op graph (van Krieken, Acar & van Harmelen 2022 survey the issue across t-norm-derived
49 neural-symbolic operators). Sutra resolves this by Lagrange-interpolating each connective
50 as a polynomial that is exact on the 3×3 Kleene grid and C^∞ elsewhere:
51

$$\begin{aligned}\text{AND}(a, b) &= \frac{1}{2}(a + b + ab - a^2 - b^2 + a^2b^2) \\ \text{OR}(a, b) &= \frac{1}{2}(a + b - ab + a^2 + b^2 - a^2b^2) \\ \text{NOT}(a) &= -a \\ \text{XOR}(a, b) &= -ab, \quad \text{XNOR}(a, b) = ab\end{aligned}$$

52 {AND, OR, NOT} is functionally complete for the Kleene fragment; XOR/XNOR col-
53 lapse to a single multiplicative term because their interpolant is zero whenever either input
54 is U and bilinear in the $\{-1, +1\}$ corners. Every Kleene-valid connective is therefore a
55 polynomial tensor-op-graph fragment, gradient-compatible, branchless, and exact on the
56 discrete-logic regime. A symbolic if-then rule built from these gates is one fused subgraph
57 that PyTorch autograd backprops through end-to-end (§3.6).

58 2. **Beta reduction to a substrate-pure tensor-op graph.** The compiler inlines stdlib operator
59 definitions, beta-reduces through bound names, then runs an algebraic-simplification pass
60 over the residual. What's left is a fused tensor-op graph (matmul / element-wise / nonlinear)
61 with no named bindings or function calls. Three concrete moves go beyond standard inlin-
62 ing + constant folding: conditionals lower to soft-mux polynomials ($\frac{1+\text{cond}}{2} a + \frac{1-\text{cond}}{2} b$)
63 so the compiled artifact has no if opcodes; Haar-orthogonal binding rotations R_{role} are
64 materialized at compile time so runtime bind is one matmul against a constant matrix;
65 canonical synthetic axes are assigned compile-time so every primitive-type read/write is a
66 known index, not a hashtable lookup. §4.2 traces this lowering stage-by-stage on a concrete
67 program; the compilation pipeline as a whole is diagrammed in Appendix J.

68 3. **Tail recursion as the loop primitive.** Loops are tail-recursive function declarations
69 (do_while, while_loop, iterative_loop, foreach_loop) whose body's return
70 NAME(args) becomes the recurrent step. Each loop compiles to a soft-halt RNN cell with
71 substrate-pure halt detection (heaviside \rightarrow cumulative monotone halt \rightarrow soft-mux state
72 freeze). The body of every loop tick is one straight-line tensor pipeline with no in-graph
73 branches; a thin Python while True: ... break driver wraps the body and terminates
74 when the halt scalar saturates (§3.4). The state vector is fixed-width across iterations, **O(1)**
75 state, **O(N) compute**, **O(N) gradient tape during training**, where N is iterations actually
76 executed.

77 4. **Synthetic-dimension rotation binding as an angular hash map.** The compiler reserves
78 a synthetic block of canonical dimensions and uses Haar-orthogonal rotations seeded from
79 the role's content hash to bind keys to slots. To the authors' knowledge this is the first use
80 of a high-dimensional rotation pattern as the substrate for a functional hash-map primitive.

81 These four primitives integrate into a single working compiler that lowers .su source to a self-
82 contained PyTorch module on CPU or CUDA. Program inputs and outputs are embeddings in the
83 substrate's vector space; a compile-time codebook (implemented with an embedded vector database,
84 §3.5) handles the convenience of source-level string literals and nearest-string output.

85 1.2 The substrate is the architecture target

86 A Sutra program is compiled for an *embedding-space architecture*, the way a C program is compiled
87 for x86 and a CUDA kernel for an NVIDIA SM. The embedding model fixes dimensionality, the
88 geometry of the semantic block, and the meaning of every basis-vector lookup; swap the model and
89 the same source recompiles to a different .sdb codebook against a different geometry. The substrate
90 need not be an LLM, it can be any network producing a dense vector representation, including
91 the hidden state of a trained model. §3.2's ESM-2 protein-LM row demonstrates this substrate-
92 agnostically.

93

94 2 Related Work

95 2.1 Vector Symbolic Architectures

96 VSA is a family of algebraic frameworks for computing with high- dimensional vectors (Kanerva
97 2009; Plate 1995; Gayler 2003). The standard VSA development assumes hypervectors drawn from
98 a controlled random distribution designed for the algebra; bind is typically Hadamard product or
99 circular convolution. Frozen LLM embedding spaces are not designed for VSA, and the textbook
100 bind operations do not always transfer cleanly to them. Rotation binding ($R_{role} @ filler$ for
101 a role-seeded Haar-random orthogonal R_{role}) is the choice that worked across the substrates we
102 tested, and is what Sutra uses today; §3.2 reports the per-substrate measurements supporting that
103 choice.

104 The closest software peer in the VSA space is **TorchHD** (Heddes et al. 2023), a PyTorch library that
105 exposes VSA primitives (bind, bundle, similarity) as tensor operations. Sutra and TorchHD differ
106 on what the user writes and what the compiler does:

- 107 • **TorchHD is a library.** The user writes Python code that calls TorchHD primitives; control
108 flow is host-side Python; there is no source-language layer above the primitives, no compile
109 step, and no algebraic reduction across primitive calls. Each primitive call is a tensor op,
110 but the program itself is a Python function with whatever control flow the user wrote.
- 111 • **Sutra is a language with a compiler.** The user writes .su source which the compiler
112 beta-reduces to a substrate-pure tensor-op graph (§1.1-2): a single straight-line graph of
113 matmul / element-wise / nonlinear ops with no Python control flow. Loops are tail-recursive
114 function declarations that lower to soft-halt RNN cells; conditionals are differentiable fuzzy
115 interpolations rather than Python if. Hash-map structure is implemented via synthetic-
116 dimension rotation, not via a host-side dictionary.

117 A second axis where Sutra differs from existing HDC software is **string I/O**. TorchHD and similar
118 libraries expose the algebra over user-supplied hypervectors; the user maintains a `dict[str, hypervector]`
119 and an explicit codebook tensor by hand. Sutra's compile-time codebook (§3.5)
120 closes that loop: every embedded string in .su source is embedded once at compile time via the
121 configured frozen LLM, stored in the project's .sdb codebook, and decoded at the program output
122 via `nearest_string`. The frozen-LLM embedding is load-bearing, random hypervectors yield a
123 working VSA algebra with no I/O story.

124 The structural differences (Sutra contains no Python, the string-to-vector map and codebook are
125 constructed by the compiler rather than by the user, and the whole program reduces to a single fused
126 tensor-op graph) are differences in artifact shape, not library speed.

127 2.2 Comparison to other neuro-symbolic languages

128 The closest neuro-symbolic-language peers are **Scallop** (Li et al. 2023, Datalog with provenance-
129 semiring differentiability), **DeepProbLog** (Manhaeve et al. 2018, ProbLog with neural predicates),
130 **Logic Tensor Networks** (Badreddine et al. 2022, first-order logic compiled to t-norm losses), and
131 **NeurASP** (Yang et al. 2020, Answer Set Programming with neural predicates). All share a two-
132 stage perception-then-reasoning shape: a neural model extracts discrete symbols from raw input,
133 and a symbolic program reasons over those symbols. Sutra’s shape is different at this architectural
134 level: the substrate is a continuous embedding space throughout, primitives operate on vectors end-
135 to-end, and the whole program (including what would be the logic program in Scallop) compiles
136 to a single fused tensor-op graph through beta reduction. There is no discrete symbolic stratum to
137 extract into or reason over; differentiability is inherited from the tensor-op graph itself, not from
138 a provenance annotation on a relational query. The two are good at different problem structures:
139 Scallop and its peers when the problem is naturally relational and perception cleanly factors out;
140 Sutra when computation is best expressed as algebra on vectors over a substrate the program reads
141 strings into and decodes strings out of.

142 The closest HDC peer with compiler infrastructure is **HDCC** (Vergés et al. 2023), a description-
143 file DSL targeting self-contained C for embedded classification, random/level hypervectors only, no
144 general control flow, scoped to classification. **TorchHD** and **OpenHD / HD Torch** are libraries with-
145 out a language-level loop primitive. To the authors’ knowledge, no published HDC system combines
146 (a) one fused tensor-op graph as compile target, (b) HDC primitives as the operations, (c) a frozen
147 externally-trained vector embedding space as the substrate, and (d) tail-recursive loops compiled to
148 soft-halt RNN cells with constant state-vector width in recursion depth. The combination is what
149 distinguishes Sutra, not any one of those properties in isolation.

150 2.3 Differentiable Programming, AOT Compilation, and Knowledge

151 Compilation

152 The closest design ancestors are partial-evaluation systems that specialize programs at compile time
153 (the Futamura projections), differentiable programming systems that treat programs as differentiable
154 functions (JAX), AOT compilation of neural networks (TVM, XLA), and knowledge compilation in
155 symbolic AI (Darwiche & Marquis 2002). Sutra differs from each: TVM/XLA start from a network,
156 not toward one; JAX treats programs as differentiable but does not bake source literals into weights;
157 partial evaluation specializes for compile-time-known values but does not target a neural-network-
158 shaped artifact; knowledge compilation targets Boolean circuits, not continuous embedding spaces.
159 Sutra’s combination (fold source literals into the weight structure, compile control flow to RNN cells,
160 run the whole program as one tensor-op graph over a *continuous* substrate) is the novel position.

161

162 3 Consolidation into Canonical Primitives

163 The central design move: hold the operation interface fixed and pick a binding implementation
164 that works on dense externally-trained substrates. Standard VSA’s Hadamard product fails here,
165 elementwise multiplication of correlated real-valued vectors produces destructive crosstalk on bun-
166 dled retrieval (§3.2 measures this directly). Rotation binding works: each role gets a Haar-random
167 orthogonal R_{role} seeded by $\text{hash}(\text{role})$, and $\text{bind}(\text{role}, \text{filler}) = R_{\text{role}} @ \text{filler}$ is
168 invertible (unbind is the transpose) and well-conditioned. The compiler caches R_{role} per-role at
169 module init so runtime bind is a single matmul against a precomputed matrix.

170 3.1 Notation

171 We work in \mathbb{R}^d with d the substrate’s embedding dimension (768 for nomic-embed-text). Every
172 value has the layout [semantic | synthetic]. The seven primitive operations: $\text{bind}(r, f) = R_r f$
173 where $R_r = \text{QR}(\text{hash}(r))$. Q is Haar-orthogonal, $\text{unbind}(r, v) = R_r^\top v$, $\text{bundle}(x, y) = (x +$
174 $y) / (\|x + y\| + \varepsilon)$, $\text{similarity}(x, y) = (x \cdot y) / (\|x\| \|y\| + \varepsilon)$, $\text{normalize}(v) = v / (\|v\| + \varepsilon)$, the
175 Lagrange Kleene gates as in §1.1-1, and the soft-halt cell of §3.4. Full signature/definition table and
176 the soft-halt cell update equations are in Appendix A.

177 3.2 Capacity of rotation versus Hadamard binding across substrates

178 We measure decode accuracy as a function of bundle width k on real embeddings across
179 four substrates spanning two modalities: three frozen LLM text encoders (nomic-embed-
180 text, all-minilm, mxbai-embed-large) and one frozen protein language model (ESM-2 small,
181 facebook/esm2_t6_8M_UR50D). LLM substrates embed an 84-word noun vocabulary; the ESM-2
182 substrate embeds an 84-sequence amino-acid vocabulary (full protocol in Appendix C). For each
183 bundle width and binding scheme we run 10 trials, sampling k random (role, filler) pairs without re-
184 placement, forming the bundle, and decoding by unbind + argmax-cosine against the full codebook.
185 *Rotation binding* uses a role-seeded Haar-orthogonal R_{role} ; *Hadamard binding* is the textbook
186 elementwise product (MAP-VSA).

187 Cross-substrate decode accuracy at representative widths (full $k \in \{2, 4, 8, 16, 24, 32, 48\}$ sweeps
188 in Appendix C):

substrate (dim)	rotation k=8	rotation k=48	Hadamard k=8	Hadamard k=48
nomic-embed-text (768)	100.0%	93.3%	87.5%	48.3%
all-minilm (384)	100.0%	42.3%	7.5%	1.7%
mxbai-embed-large (1024)	100.0%	72.1%	2.5%	1.0%
ESM-2 (320)	100.0%	44.2%	28.7%	4.2%

189 ESM-2 (Lin et al., Science 2023) is a protein language model trained on UniRef with
190 no natural-language exposure; the same rotation-vs-Hadamard pattern reproduces in that
191 modality. Rotation reversibility round-trip across all four substrates: mean $\|\text{unbind}(R,$
192 $\text{bind}(R, x)) - x\| = 1.5 \times 10^{-15}$ (floating-point round-off, Q orthogonal). Reproduction:
193 `experiments/rotation_binding_capacity_{llm,bioinformatics}.py`.

194 3.2.1 Noise accumulation across chained bind/unbind cycles

195 The §3.2 protocol measures one bind+bundle+unbind cycle. Nested records (a recovered filler be-
196 coming the role of a sub-record) add bundle noise per level. We measured this directly: chain
197 lengths $L \in \{1, 2, 4, 8, \dots\}$, 20 trials, bundle width 4. Raw accuracy holds at 100% through $L=2$ on
198 every substrate and falls to chance (1/84) by $L=8$. The demonstrated regime is therefore single-cycle
199 records, which matches the shape of the `role_filler_record`, `knowledge_graph`, and predicate-
200 lookup demos. Pure rotation chains without per-step distractor bundling remain exact (round-trip
201 1.5×10^{-15} per cycle), so the noise mechanism here does not apply to the soft-halt loop cell of §3.4.
202 Reproduction script: `experiments/crosstalk_chain.py`; full per-substrate L -sweep tables in
203 Appendix D.

204 3.3 The extended-state-vector layout

205 Every value carries a fixed [semantic | synthetic] layout: the d -dimensional semantic block
206 holds the substrate embedding for vector-shaped values, and a small synthetic block reserves canon-
207 ical axes for primitive types (real, imag, truth, char) and a loop-completion flag, with the remaining
208 axes paired into 2D Givens planes for variable slots. Default at $d = 768$ (nomic-embed-text): a 100-
209 dim synthetic block accommodates the five canonical axes plus 47 disjoint slots. Rotation binding
210 is block-diagonal across the split (Q_{role} is Haar-random in the semantic block, identity on the
211 synthetic block), so the synthetic axes pass through bind/unbind unchanged, a fuzzy-truth scalar can
212 coexist with a semantic vector inside the same value without bind smearing them. Full per-axis
213 purpose table and slot allocator details in Appendix B.

214 3.4 First-class loops as RNN cells

215 Runtime data-dependent loops compile to **self-halting RNN cells**. Each tick: snapshot pre-step
216 state, evaluate halt on the substrate (truth-axis read \rightarrow heaviside \rightarrow cumulative saturating sum to
217 halted), run the cell body, soft-mux between pre- and new-step state by halted. A Python while
218 True: driver breaks the moment halted saturates; this is the only host-side branch in the loop

219 machinery. Inside the cell body, every operation is a substrate tensor op. No compile-time iteration
 220 cap, programs terminate when their halt condition fires. Standard PyTorch tracing handles a Python
 221 while-loop wrapping pure tensor ops; autograd records each iteration as it executes, which is the
 222 mechanism §3.6 relies on for backprop through the cell. Figure~1 visualizes one tick.

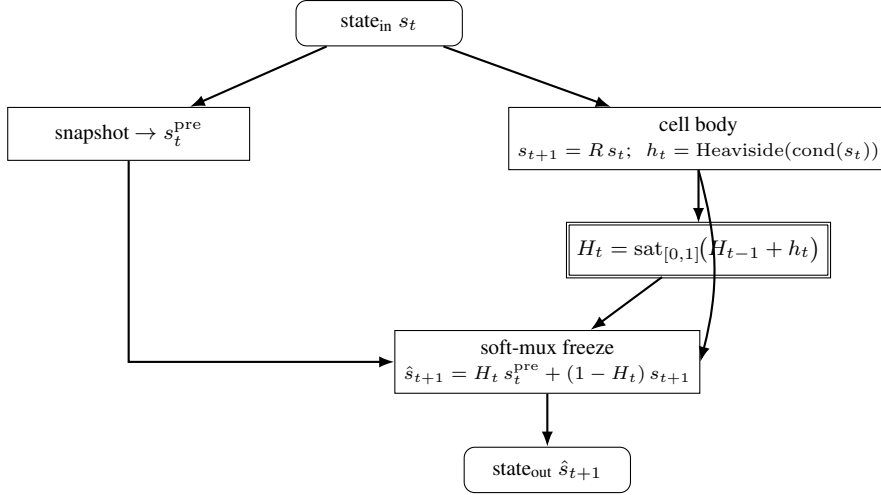


Figure 1: Per-tick dataflow of the soft-halt RNN cell. Once H_t saturates at 1, the soft-mux output equals s_t^{pre} , the loop has frozen. The cumulative halt H_t acts as a boundary read of the same shape as the codebook decode (§3.5).

223 **Constant memory in recursion depth.** The state vector is fixed-width and shared across iterations,
 224 so a tail-recursive loop consumes $O(1)$ memory in the state vector regardless of trip count. Compute
 225 is $O(N)$ and the autograd tape during training is $O(N)$ in iterations actually executed (standard Py-
 226 Torch, freed after backward). To the authors' knowledge no other HDC system or compiler exposes
 227 user-program-level recursion: HDCC is scoped to classification pipelines, TorchHD requires the
 228 user to write Python loops over hypervectors. The recurrent shape that emerges is what Siegelmann
 229 & Sontag (1992) showed computes any Turing-machine-computable function with rational weights.

230 3.5 I/O is in the embedding space; the codebook is a comfort layer

231 A Sutra program's inputs and outputs are embeddings in the substrate's vector space. Strings are a
 232 convenience for writing source-level literals: every string literal in `.su` source is embedded once
 233 at compile time and stored in a **codebook** (implemented as an embedded vector database with an
 234 HNSW index, on disk as a `.sdb` file shipped alongside the compiled module). At the program's
 235 output boundary, the runtime `decode_VSA.nearest_string(query)` maps a query embedding to
 236 the nearest stored string when the program's caller wants a string back. Calling the codebook at
 237 this boundary is shape-equivalent to calling PyTorch for a `matmul`, neither is the kind of host-side
 238 control flow substrate purity forbids. Implementation details (RDF triple layout, HNSW parameters,
 239 `.sdb` file format, complexity analysis) are in Appendix E.

240 3.6 End-to-end differentiable training through Sutra operations

241 Because every Sutra primitive compiles to a differentiable tensor operation, the compiled graph
 242 supports standard PyTorch `loss.backward()` without modification. We verify this by training
 243 learnable parameters through a fuzzy-logic classifier built entirely from Sutra operations.

244 **Setup.** 992 words across twenty semantic categories (50 each, deduplicated; full list in Appendix
 245 G) are embedded via `nomic-embed-text` (768-d, frozen). Twenty learnable prototype vectors are
 246 initialized randomly. The classifier computes cosine similarity between input and each prototype
 247 and applies a Lagrange-interpolated fuzzy if-then rule:

$$\text{rule}_i = \text{AND}\left(\text{sim}(x, p_i), \bigwedge_{j \neq i} \text{NOT}(\text{sim}(x, p_j))\right)$$

248 with the AND-of-NOTs left-folded across $K - 1$ other classes (so the $K = 20$ rule nests nineteen
249 ANDs deep). Full-batch cross-entropy over the twenty rule scores drives Adam updates (lr=0.005)
250 on the prototype embeddings.

251 **Results.** Random init: 4% accuracy (chance = 5%). Training reaches 95% by epoch 50 and holds
252 through epoch 299, loss converging to 1.154. Gradient norms at all twenty prototypes are nonzero
253 throughout (range 0.94–4.20), so backprop reaches every learnable parameter through similarity
254 \rightarrow fuzzy_not \rightarrow nineteen nested fuzzy_and \rightarrow cross-entropy.

Phase	Accuracy	Loss
Before	4%	3.01
After	95%	1.15

255 Appendix K diagrams the explicit graph for $K = 3$; the $K = 20$ graph used in the experiment has
256 the same shape with twenty learnable prototypes and the AND-of-NOTs left-folded across nineteen
257 NOT(sim) terms. The input embedding fans out to K cosine-similarity nodes against K learnable
258 prototypes; each sim_i enters one branch of an AND-tree (the i-th rule takes sim_i directly and
259 NOT(sim_j) for $j \neq i$); the K rule scores are stacked, scaled by temperature, softmaxed, and cross-
260 entropied against the label. Every node is a PyTorch tensor op, no Python branches and no string-
261 keyed lookup, and backprop reaches every learnable parameter through the same compiled graph
262 that runs at inference.

263 At K=20 the rule for class i is an AND of sim(x, proto_i) with a left-folded chain of nineteen
264 NOT(sim) terms, a tensor pipeline that could naively saturate or vanish gradients somewhere along
265 the chain. Empirically it doesn't: every prototype receives a nonzero gradient, accuracy reaches 95%
266 on a vocabulary $70\times$ larger than the K=3 setting ($15 \rightarrow 992$ words), and the symbolic program text is
267 unchanged across training. The remaining 5% gap reflects irreducible semantic overlap (e.g. *salmon*
268 fits food and color); gradient norms remain bounded above zero throughout, so this is the optimizer
269 plateauing under those overlaps, not gradient pathology. Standard torch.autograd suffices (no
270 Sutra-specific autograd machinery) because the compiler emits only operations PyTorch already
271 knows how to differentiate. Reproduction: experiments/differentiable_training.py + raw
272 JSON.

273 3.7 Type system and surface syntax

274 Sutra's surface syntax is typed: every value carries a primitive class from a fixed set (int, float,
275 complex, char, bool, fuzzy, trit, vector, matrix, permutation, map, string, scalar,
276 void), and the type drives the synthetic-axis allocation in the extended layout (Appendix B). Type
277 information is pre-compile-time annotation in the TypeScript sense: it is read by the inliner and the
278 layout pass before the tensor graph is built, but it is opinionated rather than authoritarian. A diver-
279 gent assignment warns and still emits a graph, because the runtime guarantee is mathematical not
280 structural; a type mismatch produces a semantically meaningless but mathematically valid output
281 rather than a runtime exception. The surface itself presents if / while / for / assignment forms
282 that read imperatively for ergonomic familiarity; the inliner and egglog simplifier (§4) beta-reduce
283 these into the functional tensor-op core, so the imperative-looking source is a veneer over the same
284 compiled graph a hand-written functional spec would produce.

285

286 4 The Sutra Compiler

287 The compiler is a five-stage pipeline:

- 288 1. **Lex + parse:** .su source \rightarrow AST.
- 289 2. **Inline + simplify:** stdlib operator definitions inlined; an egglog-based simplifier folds
290 equivalent expressions and runs common-subexpression elimination over the algebra.
- 291 3. **Codegen:** AST \rightarrow Python source emitting PyTorch tensor ops. The emitted module in-
292 cludes the runtime class (`_TorchVSA`) as inline source so the artifact is self-contained.

293 4. **Compile-time substrate population:** `embed_batch` fetches embeddings for ev-
294 ery string literal; `populate_sutradb` pushes the codebook into SutraDB;
295 `prewarm_rotation_cache` precomputes role rotations.
296 5. **Execute:** emitted module loaded; chosen device (CUDA or CPU) initialized at module
297 import; `main()` called; result returned.

298 The runtime class is emitted inline rather than imported because the emitted module *is* the substrate-
299 pure tensor-op graph; every compile-time decision (extended-state-vector dimensions, codebook
300 contents, role rotations, SutraDB path, optional `torch.compile`) is baked into the emitted source.
301 Stages 1–4 run at compile time and stage 5 is the runtime forward pass; Appendix J diagrams the
302 pipeline as a vertical flow with the residual at each stage.

303 4.1 Substrate-purity invariants

304 Three invariants the compiler enforces: (1) every primitive runs on the substrate (numpy is allowed
305 only at compile time for codebook construction and rotation pre-warm, never on the runtime hot
306 path); (2) no scalar extraction inside an operation: operations may not unpack a Python float from
307 a substrate vector, do scalar arithmetic, and pack the result back; (3) no Python control flow inside
308 an operation: loop halt uses substrate primitives (`heaviside`, `saturate_unit`) instead of Python
309 ternaries.

310 4.2 Compile-time resolution of role rotations

311 The central compile-time mechanism that lets the compiler emit a substrate-pure tensor-op
312 graph is **precomputed rotation matrices**: every role rotation is constructed at compile time
313 (`prewarm_rotation_cache`) and stored as a constant tensor. At runtime, `bind(role, filler)`
314 is a single matmul against a precomputed matrix, the compile-time resolution eliminates the QR con-
315 struction from the runtime graph entirely. Role rotations are runtime constants, like neural-network
316 weights at inference; opt-in `torch.compile` (`SUTRA_TORCH_COMPILE=1`) further folds the per-tick
317 loop body into a single fused kernel. Appendix F traces the lowering of `encode2(r_a, f_a, r_b,`
318 `f_b) := bundle(bind(r_a, f_a), bind(r_b, f_b))` through every reduction stage; the bot-
319 tom of the chain contains no `bind/bundle/normalize` symbol and no Python control flow, so
320 surface lambda calculus and runtime tensor arithmetic are two notations for the same computation.

321

322 5 Demonstration, limitations, and future work

323 The smoke test (`examples/_smoke_test.py`) runs 10 demonstration programs end-to-end across
324 27 .su files (Appendix I); loop coverage lives in `examples/do_while_adder.su` and the 23-case
325 `test_loop_function_decl.py` suite, and the §3.6 differentiable- training experiment uses the
326 same primitive set. The embedded codebook covers the compile-time `embed` → runtime `decode`
327 path; extended features (hashmap routing, persistent codebook via `SUTRA_DB_PATH`) are deferred
328 pending a concrete requirement.

329

330 6 Conclusion

331 Sutra compiles a typed pure-functional source language to a substrate-pure PyTorch tensor-op graph:
332 one vector layout per value, one tensor op per primitive, one dataflow graph per program, no type
333 dispatch at the leaves. With the language in hand, asking which embedding operations compose at
334 what capacity on which substrates becomes a program to write.

335

336 **References**

337 • Darwiche, A., & Marquis, P. (2002). A knowledge compilation map. *JAIR* 17:229–264.
338 • Gayler, R. W. (2003). Vector symbolic architectures answer Jackendoff's challenges for
339 cognitive neuroscience. *Joint International Conference on Cognitive Science*.
340 • Kanerva, P. (2009). Hyperdimensional computing: An introduction to computing in dis-
341 tributed representation with high-dimensional random vectors. *Cognitive Computation*
342 1(2):139–159.
343 • Kleene, S. C. (1952). *Introduction to Metamathematics*. North- Holland. The strong three-
344 valued logic system used as the ground for Sutra's polynomial fuzzy connectives (§1.1-1).
345 • Badreddine, S., Garcez, A. d., Serafini, L., & Spranger, M. (2022). Logic Tensor Networks.
346 *Artificial Intelligence* 303.
347 • Hájek, P. (1998). *Metamathematics of Fuzzy Logic*. Trends in Logic vol. 4. Kluwer
348 Academic. The standard reference for t-norm-based fuzzy logics (Gödel, Łukasiewicz,
349 product) cited in §1.1-1 to place Sutra's polynomial connectives.
350 • Heddes, M., Nunes, I., Vergés, P., Kleyko, D., Abraham, D., Givargis, T., Nicolau, A.,
351 & Veidenbaum, A. (2023). Torchhd: An open source python library to support research
352 on hyperdimensional computing and vector symbolic architectures. *Journal of Machine*
353 *Learning Research* 24(255):1–10.
354 • Li, Z., Huang, J., & Naik, M. (2023). Scallop: A Language for Neurosymbolic Pro-
355 gramming. *Proceedings of the ACM on Programming Languages* 7(PLDI):1463–1487.
356 arXiv:2304.04812.
357 • Manhaeve, R., Dumancic, S., Kimmig, A., Demeester, T., & De Raedt, L. (2018). Deep-
358 ProbLog: Neural Probabilistic Logic Programming. *NeurIPS*.
359 • Serafini, L. & Garcez, A. d. (2016). Logic Tensor Networks: Deep Learning and Logical
360 Reasoning from Data and Knowledge. *NeSy Workshop*.
361 • van Krieken, E., Acar, E., & van Harmelen, F. (2022). Analyzing Differentiable Fuzzy
362 Logic Operators. *Artificial Intelligence* 302:103602. The differentiable-fuzzy-logic sur-
363 vey cited in §1.1-1; analyzes t-norm-derived AND/OR/IMPLIES operators in the neural-
364 symbolic context and is the closest prior literature to Sutra's polynomial approach.
365 • Vergés, P., Heddes, M., Nunes, I., Givargis, T., & Nicolau, A. (2023). HDCC: A Hy-
366 perdimensional Computing compiler for classification on embedded systems and high-
367 performance computing. arXiv:2304.12398.
368 • Yang, Z., Ishay, A., & Lee, J. (2020). NeurASP: Embracing Neural Networks into Answer
369 Set Programming. *IJCAI*.
370 • Plate, T. A. (1995). Holographic reduced representations. *IEEE Transactions on Neural*
371 *Networks* 6(3):623–641.
372 • Siegelmann, H. T. & Sontag, E. D. (1992). On the computational power of neural nets.
373 *COLT '92*. Establishes that recurrent neural networks with rational weights are Turing-
374 complete; the result Sutra inherits via tail-recursive loops over a fixed-width state vector.
375 • Smolensky, P. (1990). Tensor product variable binding and the representation of symbolic
376 structures in connectionist systems. *Artificial Intelligence* 46(1–2):159–216.

377

378 **Appendix**

379 **Appendix A. Notation: extended layout and primitive operations**

380 We work in a fixed-dimensional real vector space \mathbb{R}^d where d is the substrate's embedding dimension
 381 (768 for nomic-embed-text, 384 for all-minilm, 1024 for mxbai-embed-large, 320 for ESM-2). Ev-
 382 ery Sutra value carries the extended layout [semantic | synthetic], a d -dimensional semantic block
 383 holding the substrate embedding, concatenated with a small fixed-width synthetic block reserving
 384 canonical axes for primitive types (real, imag, truth, char, loop-done) and slot machinery (§3.3).
 385 Where notation does not distinguish, "vector" means "the full extended-layout tensor."

386 The seven primitive operations are:

$$\begin{aligned} \text{bind}(r, f) &= R_r f, & R_r &= \text{QR}(\text{seed} = \text{hash}(r)).Q \\ \text{unbind}(r, v) &= R_r^\top v \\ \text{bundle}(x, y) &= \frac{x + y}{\|x + y\| + \varepsilon} \\ \text{similarity}(x, y) &= \frac{x \cdot y}{\|x\| \|y\| + \varepsilon} \\ \text{normalize}(v) &= \frac{v}{\|v\| + \varepsilon} \end{aligned}$$

387 plus the Lagrange Kleene gates (scalar \rightarrow scalar, exact on the $\{-1, 0, +1\}^2$ grid, §1.1-1) and the
 388 soft-halt cell (state, halt \rightarrow state', halt', §3.4).

389 The Lagrange gates in closed form:

$$\begin{aligned} \text{AND}(a, b) &= \frac{1}{2}(a + b + ab - a^2 - b^2 + a^2b^2) \\ \text{OR}(a, b) &= \frac{1}{2}(a + b - ab + a^2 + b^2 - a^2b^2) \\ \text{NOT}(a) &= -a \\ \text{XOR}(a, b) &= -ab \\ \text{XNOR}(a, b) &= ab \end{aligned}$$

390 The soft-halt cell update is, in compact form,

$$\begin{aligned} s_{t+1} &= R s_t && \text{(rotation step)} \\ h_t &= \text{Heaviside}(\text{cond}(s_t)) && \text{(per-tick halt signal)} \\ H_t &= \text{sat}_{[0,1]} \left(\sum_{k \leq t} h_k \right) && \text{(cumulative monotone halt)} \\ \hat{s}_{t+1} &= H_t s_t + (1 - H_t) s_{t+1} && \text{(soft-mux freeze)} \end{aligned}$$

391 Every right-hand side is a tensor expression with no Python control flow. The compile-time primi-
 392 tives `RotationFor` and `embed` produce constants R_r and basis vectors at compile time and are not
 393 part of the runtime tensor graph.

394 **Appendix B. Extended-state-vector layout: per-axis assignments**

395 §3.3 describes the [semantic | synthetic] layout in prose. The diagram and per-axis purpose
 396 table below give the concrete allocation referenced in `codegen_pytorch.py`:

	+-----+-----+-----+-----+-----+
value	semantic block R I T C L slots...
	+-----+-----+-----+-----+-----+

```

400 |<-- semantic_dim ----->|<--- synthetic_dim ----->|>
401         0   1   2   3   4   5..
402         REAL IMAG TRUTH CHAR LOOP_DONE
403                                _FLAG

```

Index	Purpose
synthetic[0]	AXIS_REAL (real component for int/float/complex)
synthetic[1]	AXIS_IMAG (imaginary component for complex)
synthetic[2]	AXIS_TRUTH (fuzzy truth scalar; bool/comparisons)
synthetic[3]	AXIS_CHAR_FLAG (marks char primitives)
synthetic[4]	AXIS_LOOP_DONE (substrate-side completion flag)
synthetic[5..]	SLOT_BASE: disjoint 2D Givens slots for variable storage

404 At semantic_dim = 768 (nomic-embed-text), synthetic_dim = 100 accommodates the five
405 canonical axes plus 47 disjoint Givens slots.

406 **Appendix C. Capacity: full per-substrate sweeps**

407 Cross-substrate decode accuracy at full bundle widths $k \in \{2, 4, 8, 16, 24, 32, 48\}$. The four
408 substrates use 84-entry vocabularies (LLM substrates: 84-word noun set spanning animals, foods,
409 objects, places, abstract nouns; ESM-2: 84-sequence amino-acid set covering canonical signal pep-
410 tides, cell-penetrating peptides, antimicrobial peptides, classic affinity-tag motifs, and deterministic
411 random k-mers). All embeddings are unit-normalized; nomic-embed-text and ESM-2 are addition-
412 ally mean-centered.

413 **nomic-embed-text (768-d, mean-centered):**

k	rotation accuracy	rotation signal cos	Hadamard accuracy	Hadamard signal cos
2	100.0%	+0.703	95.0%	+0.488
4	100.0%	+0.497	95.0%	+0.400
8	100.0%	+0.354	87.5%	+0.307
16	100.0%	+0.251	84.4%	+0.230
24	100.0%	+0.203	60.8%	+0.189
32	99.1%	+0.176	63.1%	+0.167
48	93.3%	+0.144	48.3%	+0.136

414 **all-minilm (384-d):**

k	rotation accuracy	rotation signal cos	Hadamard accuracy	Hadamard signal cos
2	100.0%	+0.711	45.0%	+0.386
4	100.0%	+0.506	10.0%	+0.335
8	100.0%	+0.356	7.5%	+0.315
16	92.5%	+0.252	3.1%	+0.299
24	76.2%	+0.203	2.9%	+0.300
32	66.9%	+0.179	2.5%	+0.297
48	42.3%	+0.144	1.7%	+0.294

415 **mxbai-embed-large (1024-d):**

k	rotation accuracy	rotation signal cos	Hadamard accuracy	Hadamard signal cos
2	100.0%	+0.708	15.0%	+0.311
4	100.0%	+0.500	2.5%	+0.304
8	100.0%	+0.353	2.5%	+0.295
16	98.8%	+0.251	1.2%	+0.294
24	95.8%	+0.203	0.8%	+0.293
32	85.3%	+0.176	0.9%	+0.292
48	72.1%	+0.146	1.0%	+0.291

416 **ESM-2 small protein language model (320-d, mean-centered):**

k	rotation accuracy	rotation signal cos	Hadamard accuracy	Hadamard signal cos
2	100.0%	+0.713	75.0%	+0.470
4	100.0%	+0.501	50.0%	+0.323
8	100.0%	+0.349	28.7%	+0.257
16	90.6%	+0.252	16.2%	+0.185
24	77.1%	+0.205	11.2%	+0.171
32	61.9%	+0.174	6.2%	+0.141
48	44.2%	+0.143	4.2%	+0.117

417 The signal cosine for Hadamard is comparable to rotation's, but the noise floor is much higher be-
418 cause the elementwise product of correlated real-valued embeddings produces a result that overlaps
419 with many distractors in the codebook rather than near-orthogonally with one.

420 **Appendix D. Crosstalk depth: full per-substrate L-sweep**

421 The §3.2.1 protocol: chain length $L \in \{1, 2, 4, 8, 16, 32\}$, 20 trials, bundle width 4 (3 distractors
422 per cycle). Forward-bind through L role rotations bundling 3 distractor (role, filler) pairs at each
423 step; unbind in reverse and decode. Two flavors: *raw* (no cleanup) and *snap* (argmax-cosine cleanup
424 against the codebook after each unbind step).

substrate	L=1 raw	L=2 raw	L=4 raw	L=1 snap	L=2 snap	L=4 snap
nomic-embed-text	100%	100%	20%	100%	10%	0%
all-minilm	100%	100%	5%	100%	0%	0%
mxbai-embed-large	100%	100%	5%	100%	0%	0%

425 By chain length 8 raw accuracy is at chance (1/84) on all three substrates. Snap is *worse* than
426 raw past chain length 1: a hard codebook commitment converts soft noise into a high-confidence
427 wrong answer that the next unbind cannot recover from. The runtime does not implicitly snap
428 between operations; cleanup is an explicit step the program schedules where it knows the codebook
429 is the right reference. Reproduction script: `experiments/crosstalk_chain.py`; raw JSON in
430 `experiments/crosstalk_chain_results.json`.

431 **Appendix E. Codebook implementation details**

432 The §3.5 codebook is implemented as an embedded vector database (internally SutraDB) shipped
433 as part of the compiler, analogous to SQLite being embedded in an application rather than run as
434 a separate service. The data model is RDF triples with f32-vector literals as the object position,
435 indexed by a built-in HNSW index for nearest-neighbor decode. The on-disk format is a `.sdb` file
436 that travels alongside the compiled Python module; no external service, no separate install, no net-
437 work dependency. Every embedded string in a Sutra program is inserted with the embedding as the
438 object of a triple typed `<http://sutra.dev/f32vec>`. Strings declared but unused in expressions

439 are still inserted, so they remain decodable. The compiled module's Python data section never carries the embeddings, they live in the .sdb file, an artifact of compilation, not a service the runtime contacts.

442 nearest_string runs over an HNSW (Hierarchical Navigable Small World) approximate-nearest-neighbor graph maintained by the triplestore. HNSW (Malkov & Yashunin, TPAMI 2020) has **O(log N) expected and worst-case query time** under standard graph-construction parameters; it has displaced linear scan as the default ANN index in Faiss, Milvus, Weaviate, Qdrant, and most production vector databases. A 100-string codebook and a 100,000-string codebook have comparable decode latency at runtime, modulo HNSW's tunable M (graph degree) and ef_search (beam width); the cost difference is roughly one extra graph hop per $10\times$ growth in N.

449 Appendix F. Worked lowering of a two-field bundled record

450 The body §4.2 sketches the lowering of $\text{encode2}(r_a, f_a, r_b, f_b) := \text{bundle}(\text{bind}(r_a, f_a), \text{bind}(r_b, f_b))$. Here we trace each stage with the explicit residual.

452 **Stage 1: AST after parse.** A tree of Call nodes over named identifiers: $\text{Call}(\text{"bundle"}, \text{Call}(\text{"bind"}, r_a, f_a), \text{Call}(\text{"bind"}, r_b, f_b))$.

454 **Stage 2: beta reduction by stdlib inlining.** bind, bundle, and normalize are stdlib functions: $\text{bind}(r, f) \equiv \text{RotationFor}(r) f$, $\text{bundle}(x, y) \equiv \text{normalize}(x + y)$, $\text{normalize}(v) \equiv v / (\|v\| + \varepsilon)$. After substitution the body becomes

$$\text{normalize}(\text{RotationFor}(r_a) f_a + \text{RotationFor}(r_b) f_b).$$

457 No bind or bundle symbol remains; the residual is straight-line algebra over four tensor primitives.

458 **Stage 3: compile-time constant resolution.** $\text{RotationFor}(r)$ is a compile-time function returning $R = \text{QR}(\text{seed} = \text{hash}(r)).Q$. The compiler evaluates it for each role at compile time, freezes the results as constant tensors R_a and R_b , and stores them in the rotation cache. The body becomes $\text{normalize}(R_a f_a + R_b f_b)$, R_a and R_b are now load-bearing constants in the same sense as the weight matrices of a feed-forward network.

463 **Stage 4: peephole fusion.** The simplifier recognizes $\text{normalize}(\sum_i R_i f_i)$ as the bundle-of-binds pattern and rewrites it to $\text{_VSA.bundle_of_binds}([(R_a, f_a), (R_b, f_b)])$, one kernel launch instead of two matmuls + add + norm.

466 **Stage 5: leaf tensor ops at runtime.** bundle_of_binds stacks rotations into a (k, d, d) tensor, stacks fillers into (k, d) , runs one batched einsum + sum + L2-normalize:

$$v = \sum_k R_k f_k = \text{einsum}(\text{"kij,kj->i"}, \text{stack}([R_a, R_b]), \text{stack}([f_a, f_b]))$$

$$\text{encode2} = v / (\|v\| + \varepsilon)$$

468 The compiled forward pass for encode2 is exactly those three torch calls (einsum, linalg.norm, divide) over precomputed R_a, R_b and runtime-supplied f_a, f_b .

470 Appendix G. §3.6 differentiable-training vocabulary

471 Twenty categories of fifty words each (992 unique after deduplication), embedded via nomic-embed-text:

- 473 • **animal:** dog, cat, bird, fish, horse, lion, tiger, elephant, rabbit, monkey, bear, wolf, fox, deer, mouse, snake, frog, turtle, dolphin, whale, shark, eagle, owl, sparrow, crow, robin,
- 474 parrot, swan, duck, goose, chicken, cow, pig, sheep, goat, donkey, camel, giraffe, kangaroo,
- 475 koala, panda, leopard, cheetah, hippopotamus, rhinoceros, antelope, buffalo, hedgehog,
- 476 squirrel, raccoon
- 477 • **vehicle:** car, truck, airplane, boat, bicycle, motorcycle, bus, train, ship, helicopter, tractor,
- 478 scooter, van, taxi, jeep, sailboat, kayak, canoe, raft, submarine, glider, jet, rocket, space-
- 479 ship, sled, skateboard, wagon, carriage, chariot, ambulance, firetruck, limousine, minivan,
- 480

481 hatchback, sedan, coupe, convertible, pickup, trailer, ferry, yacht, dinghy, blimp, balloon,
482 hovercraft, tram, moped, tricycle, rollerblade, unicycle

- 483 • **food:** apple, bread, cheese, rice, pasta, banana, salad, soup, meat, pizza, sandwich, burger,
484 taco, sushi, cake, cookie, pie, donut, muffin, pancake, waffle, bagel, croissant, omelet,
485 salmon, tuna, beef, pork, lamb, bacon, ham, sausage, steak, lobster, shrimp, crab, oyster,
486 clam, broccoli, carrot, lettuce, tomato, potato, cucumber, onion, garlic, pepper, eggplant,
487 spinach, mushroom
- 488 • **color:** red, blue, green, yellow, orange, purple, black, white, brown, pink, gray, cyan,
489 magenta, violet, indigo, turquoise, teal, lavender, maroon, crimson, scarlet, ruby, gold,
490 silver, bronze, copper, beige, tan, ivory, charcoal, navy, sapphire, emerald, jade, olive,
491 lime, mint, coral, peach, plum, mauve, fuchsia, amber, ochre, sienna, mahogany, chocolate,
492 caramel, mustard, azure
- 493 • **clothing:** shirt, pants, dress, hat, shoes, jacket, socks, gloves, scarf, belt, sweater, hoodie,
494 jeans, shorts, skirt, blouse, coat, cap, beanie, mittens, tights, leggings, vest, blazer, suit,
495 tuxedo, gown, robe, kimono, kilt, poncho, cloak, cape, sneakers, boots, sandals, slip-
496 pers, heels, loafers, tie, bowtie, cufflinks, watch, ring, necklace, earrings, bracelet, anklet,
497 brooch, headband
- 498 • **weather:** rain, snow, wind, cloud, storm, fog, frost, hail, thunder, lightning, drizzle, down-
499 pour, blizzard, hurricane, tornado, cyclone, typhoon, sleet, mist, haze, smog, sunshine,
500 sunlight, sunset, sunrise, dawn, dusk, twilight, breeze, gust, gale, humidity, drought, flood,
501 monsoon, snowfall, snowstorm, rainstorm, sandstorm, heatwave, chill, dew, hailstorm,
502 thaw, overcast, sunny, cloudy, rainy, snowy, windy
- 503 • **emotion:** joy, sadness, anger, fear, love, hope, surprise, disgust, pride, envy, happiness,
504 grief, rage, anxiety, affection, despair, delight, shame, guilt, confidence, contentment, jeal-
505 ously, regret, sorrow, frustration, satisfaction, awe, wonder, gratitude, compassion, sym-
506 pathy, empathy, irritation, boredom, excitement, enthusiasm, calm, serenity, melancholy,
507 nostalgia, longing, embarrassment, humiliation, indifference, ecstasy, bliss, dread, terror,
508 amusement, loneliness
- 509 • **tool:** hammer, saw, drill, wrench, screwdriver, knife, scissors, pliers, axe, shovel, rake, hoe,
510 spade, pickaxe, crowbar, mallet, chisel, sander, level, ruler, vise, clamp, ratchet, socket,
511 awl, scraper, trowel, broom, mop, sponge, bucket, ladder, jackhammer, sledgehammer,
512 paintbrush, roller, stapler, tongs, tweezers, calipers, magnifier, flashlight, multimeter, wire-
513 cutter, hacksaw, router, torch, soldering_iron, drillbit, screwbit
- 514 • **instrument:** guitar, piano, drum, violin, flute, trumpet, saxophone, harp, cello, clarinet,
515 banjo, mandolin, ukulele, harmonica, accordion, organ, keyboard, synthesizer, xylophone,
516 tambourine, maracas, bongos, marimba, vibraphone, glockenspiel, bagpipes, oboe, bas-
517 soon, trombone, tuba, lute, sitar, koto, zither, dulcimer, cymbal, gong, triangle, cowbell,
518 snare, kettledrum, recorder, piccolo, fife, didgeridoo, theremin, viola, double_bass, fiddle,
519 ocarina
- 520 • **profession:** doctor, teacher, lawyer, engineer, nurse, chef, artist, scientist, farmer, plumber,
521 electrician, carpenter, mechanic, pilot, sailor, soldier, judge, journalist, writer, poet, painter,
522 sculptor, musician, actor, dancer, singer, photographer, architect, dentist, surgeon, pharma-
523 cist, veterinarian, librarian, accountant, banker, broker, programmer, designer, manager,
524 secretary, butcher, baker, gardener, tailor, jeweler, barber, chemist, biologist, physicist,
525 mathematician
- 526 • **body_part:** head, hand, foot, eye, ear, nose, mouth, leg, arm, finger, toe, knee, elbow,
527 shoulder, hip, neck, back, chest, stomach, heart, brain, lung, liver, kidney, bone, muscle,
528 skin, hair, throat, jaw, chin, cheek, forehead, eyebrow, eyelash, lip, tongue, palm, wrist,
529 ankle, thumb, heel, spine, rib, scalp, nostril, gum, knuckle, tendon, vein
- 530 • **plant:** tree, flower, grass, bush, vine, fern, moss, herb, weed, leaf, stem, branch, bark,
531 blossom, petal, oak, maple, willow, birch, cedar, bamboo, cactus, rose, tulip, daisy, lily,
532 sunflower, orchid, ivy, basil, rosemary, thyme, sage, lavender, dandelion, clover, lotus,
533 magnolia, sycamore, redwood, baobab, eucalyptus, juniper, hemlock, fir, spruce, ash, elm,
534 poplar, chestnut
- 535 • **furniture:** chair, table, sofa, bed, desk, shelf, drawer, cabinet, wardrobe, dresser, night-
536 stand, ottoman, bench, stool, recliner, futon, couch, armchair, bookcase, sideboard, buffet,
537 cupboard, hutch, vanity, headboard, footboard, mattress, pillow, cushion, blanket, quilt,
538 comforter, lamp, mirror, rug, carpet, curtain, blind, shutter, hammock, cradle, crib, bassinet,
539 highchair, rocker, loveseat, settee, divan, chaise, headrest

- 540 • **building**: house, apartment, mansion, cottage, cabin, hut, igloo, tent, palace, castle,
- 541 fortress, tower, skyscraper, office, factory, warehouse, store, mall, restaurant, hotel, mo-
- 542 tel, hospital, school, university, library, museum, theater, stadium, arena, church, temple,
- 543 mosque, synagogue, cathedral, chapel, monastery, abbey, barn, shed, garage, basement,
- 544 attic, cellar, lobby, lounge, hallway, corridor, atrium, foyer, balcony
- 545 • **country**: France, Germany, Italy, Spain, Portugal, England, Scotland, Ireland, Norway,
- 546 Sweden, Finland, Denmark, Iceland, Russia, Poland, Greece, Turkey, Egypt, Morocco, Al-
- 547 geria, Kenya, Nigeria, Ethiopia, Ghana, Senegal, Mali, Sudan, Uganda, Tanzania, Mada-
- 548 gascar, China, Japan, Korea, Vietnam, Thailand, Malaysia, Indonesia, India, Pakistan,
- 549 Bangladesh, Iran, Iraq, Israel, Lebanon, Australia, Canada, Mexico, Brazil, Argentina,
- 550 Chile
- 551 • **sport**: football, basketball, baseball, soccer, tennis, golf, hockey, rugby, cricket, volley-
- 552 ball, swimming, running, cycling, skiing, snowboarding, surfing, sailing, rowing, kayaking,
- 553 climbing, hiking, boxing, wrestling, fencing, archery, shooting, fishing, hunting, polo, bad-
- 554 minton, ping_pong, squash, racquetball, lacrosse, handball, dodgeball, kickball, gymnas-
- 555 tics, diving, weightlifting, judo, karate, taekwondo, sumo, marathon, triathlon, decathlon,
- 556 biathlon, skating, bowling
- 557 • **drink**: water, juice, milk, tea, coffee, soda, beer, wine, whiskey, vodka, rum, gin, tequila,
- 558 brandy, cognac, champagne, cocktail, smoothie, milkshake, lemonade, cider, ale, lager,
- 559 stout, bourbon, scotch, sake, mead, punch, eggnog, kombucha, kefir, espresso, latte, cap-
- 560 puccino, mocha, americano, macchiato, frappe, hot_chocolate, cordial, shake, slushie,
- 561 syrup, fizz, brew, tonic, infusion, ginger_ale, root_beer
- 562 • **metal**: gold, silver, copper, iron, steel, aluminum, brass, bronze, tin, lead, zinc, nickel, plat-
- 563 inum, titanium, chromium, mercury, magnesium, lithium, sodium, potassium, calcium, ura-
- 564 nium, plutonium, palladium, tungsten, vanadium, cobalt, manganese, beryllium, gallium,
- 565 indium, antimony, bismuth, cadmium, cerium, neodymium, osmium, rhodium, ruthenium,
- 566 tantalum, thallium, thorium, yttrium, scandium, hafnium, niobium, molybdenum, rhenium,
- 567 iridium, rubidium
- 568 • **shape**: circle, square, triangle, rectangle, oval, ellipse, pentagon, hexagon, octagon, dia-
- 569 mond, rhombus, trapezoid, parallelogram, polygon, sphere, cube, cylinder, cone, pyramid,
- 570 prism, cuboid, tetrahedron, dodecahedron, icosahedron, octahedron, torus, helix, spiral,
- 571 crescent, star, heart, arrow, cross, line, curve, arc, ring, loop, knot, dot, vertex, edge, angle,
- 572 parabola, hyperbola, sine, wave, zigzag, scallop, annulus
- 573 • **fabric**: cotton, wool, silk, linen, polyester, nylon, denim, leather, suede, velvet, satin, lace,
- 574 tweed, cashmere, mohair, fleece, fur, canvas, burlap, jute, flannel, chiffon, organza, taffeta,
- 575 brocade, damask, paisley, gingham, plaid, herringbone, corduroy, microfiber, spandex, ly-
- 576 cra, rayon, viscose, acrylic, polypropylene, jersey, knit, sherpa, gabardine, twill, muslin,
- 577 gauze, mesh, vinyl, tulle, georgette, voile

578 Appendix H. Reproduction details and hyperparameters

579 Per-experiment configuration. All scripts live under `experiments/` in the source repository; each
 580 writes a JSON results file to the same directory on completion. RNG seeds are fixed in the source
 581 files cited; re-running reproduces the numbers reported in the body to the precision reported.

Experiment	§	Script	Trials / k	Embedding	Optimizer	Seed
Rotation vs Hadamard, LLM	3.2	<code>rotation_bin10/llg_capacity_minilm.py</code>	10/1k	minilm-embed-text, all-minilm, mxbai-embed-large		per-script
Rotation vs Hadamard, ESM-2	3.2	<code>rotation_bin10/llg_capacity_esm2_minilm.py</code>	10/1k	facebook/esm2_minilm		PR50029, 2718
Crosstalk depth	3.2.1	<code>crosstalk_c20/ll.py</code>	20/1k	three LLM substrates		per-script

Experiment §	Script	Trials / k	Embedding	Optimizer	Seed
Differentiable 3.6 training	differentiable-training.py	300 epochs	topic-embed-text (frozen)	Adam, lr=0.005	42

582 The differentiable-training run loads twenty learnable prototype vectors (initialized via
583 `torch.randn × 0.1`) and minimizes full-batch cross-entropy over the 992-word vocabu-
584 lary of Appendix G. Vocabulary embeddings are precomputed once and cached to
585 `.diff_train_embeddings.pt` (3.3 MB) so subsequent runs skip the embed step. Out-
586 put: weights → `differentiable_training_weights.pt` (3.3 MB), per-epoch metrics →
587 `differentiable_training_results.json`.

588 Hardware used for the numbers in the body: CPU torch on a single laptop (no CUDA). The full §3.6
589 run completes in ~3 min wall-clock; the §3.2 capacity sweeps complete in ~2 min per substrate;
590 the §3.2.1 crosstalk sweep completes in ~5 min. Re-running on CUDA should reproduce the same
591 accuracy numbers since the operations are deterministic given a seed.

592 Appendix I. Demonstration corpus

593 The smoke test (`examples/_smoke_test.py`) compiles and runs ten `.su` programs end-to-end
594 and asserts each output against a hardcoded expected value. The programs collectively exercise the
595 language features the body claims, with no Python control flow on the runtime path:

Program	Feature exercised
<code>hello_world.su</code>	embed + retrieve (minimal program)
<code>fuzzy_branching.su</code>	weighted-superposition conditional
<code>role_filler_record.su</code>	bind / bundle / unbind on a 3-field record (§2.1)
<code>classifier.su</code>	cosine-similarity classifier over a small codebook
<code>analogy.su</code>	associative pair memory: capital → country recovery via unbind
<code>knowledge_graph.su</code>	(subject, relation, object) triple encode + decode
<code>predicate_lookup.su</code>	bind-keyed dictionary read
<code>fuzzy_dispatch.su</code>	Lagrange-Kleene-gated dispatch among handlers
<code>nearest_phrase.su</code>	top-1 phrase retrieval over a <code>.sdb</code> codebook
<code>sequence.su</code>	foreach reduction over a list

596 Loop coverage lives in `examples/do_while_adder.su` and the 23-case
597 `tests/test_loop_function_decl.py` suite. The §3.6 differentiable-training experiment
598 uses the same primitive set the smoke-test programs are built from, no Sutra-runtime extensions,
599 just compilation of `.su` source to PyTorch tensor ops.

600 Appendix J. Compilation pipeline diagram

601 The five stages of §4 visualized as a vertical flow with the residual artifact at each stage. Stages
602 (1)–(4) run at compile time; the dashed line marks the compile/runtime boundary; stage (5) is the
603 runtime forward pass.

604 Appendix K. K=3 rule pipeline diagram

605 The explicit pipeline graph for the §3.6 differentiable-training classifier at K=3, the smallest setting
606 that exhibits the AND / AND-of-NOTs / softmax / cross-entropy shape that scales unchanged to
607 K=20.

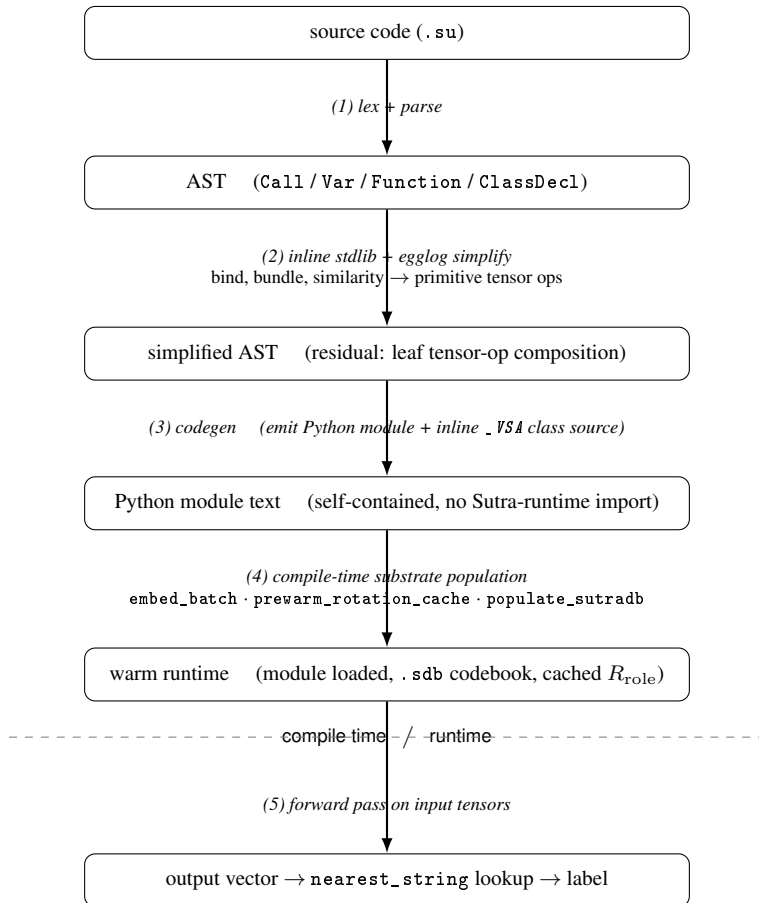


Figure 2: Five-stage compilation pipeline (§4). Boxes are intermediate artifacts; italic labels are the compiler passes that connect them.

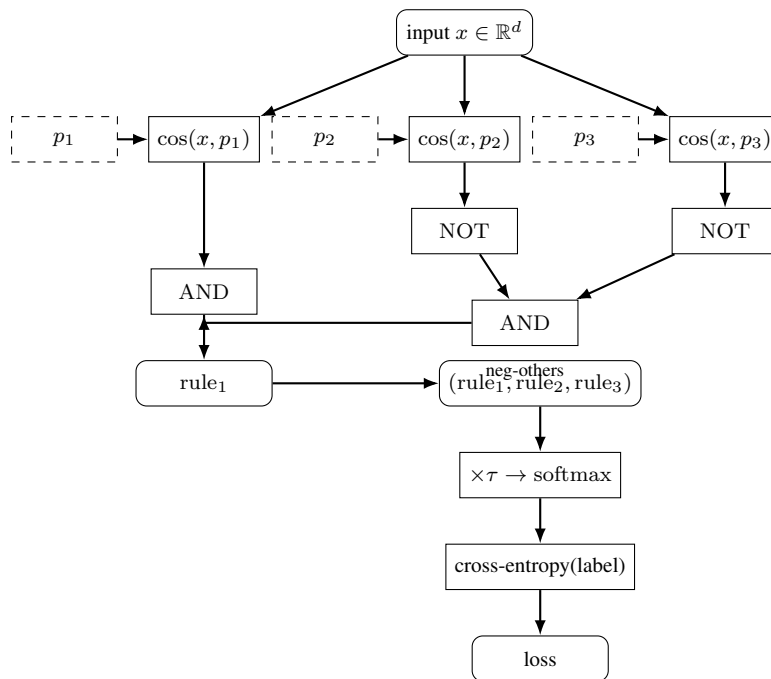


Figure 3: The $K = 3$ rule pipeline. Solid boxes are PyTorch tensor ops; dashed boxes are learnable prototypes. The AND in the leftmost branch combines $\cos(x, p_1)$ with the AND-of-NOTs over the other classes; rule_2 and rule_3 (omitted for clarity) have the symmetric shape. Every edge is a tensor; backprop reaches each p_i through this graph.